An Improved Empirical Potential Energy Function for Molecular Simulations of Phospholipids

Scott E. Feller

Department of Chemistry, Wabash College, Crawfordsville, Indiana 47933

Alexander D. MacKerell, Jr.*

Department of Pharmaceutical Sciences, School of Pharmacy, University of Maryland, Baltimore, Maryland 21201

Received: March 1, 2000; In Final Form: June 9, 2000

Improvements in the CHARMM all-atom force field for atomic-level molecular simulations of lipids are reported. Substantial adjustments have been made to the Lennard-Jones (LJ) hydrocarbon and torsional parameters and to the partial atomic charges and torsional parameters of the phosphate moiety. These changes were motivated by a combination of unexpected simulation results and recent high-level ab initio quantum mechanical calculations. The parameter optimization procedure is described, and the resulting energy function validated by an 11 ns molecular dynamics simulation of a hydrated phospholipid bilayer. Of note is the influence of the hydrocarbon LJ parameters on the conformational properties of the aliphatic tails, emphasizing the importance of obtaining the proper balance between the bonded and nonbonded portions of the force field. Compatibility with the CHARMM all-atom parameter sets for proteins and nucleic acids has been maintained such that high quality simulations of biologically interesting membranes are possible. The complete force field is included as Supporting Information and is available from www.pharmacy.umaryland.edu/∼alex.

Introduction

Computer simulation of lipid bilayers is a rapidly growing field that is benefiting immensely from improvements in hardware and algorithms. For lipid simulations, an especially important advancement is the Particle Mesh Ewald (PME)[1] algorithm for the fast and accurate calculation of the Coulombic forces that substantially determine the interaction of lipid headgroups with each other and with the solvent layer. Another key methodological improvement was the introduction of constant pressure algorithms that allow the size and shape of the simulation cell to adjust against the pressure and/or surface tension appropriate for modeling experimentally studied systems.[2,3]

Both of these developments have important implications for the optimization of potential energy parameters. In the case of Coulombic interactions, results obtained during the optimization of potential energy parameters may not be reproduced when, for example, force truncation is eliminated by use of the PME algorithm. Alternatively, the use of constant pressure methods requires that the parameters reproduce the experimental density of the system, where previously the system density was set by the fixed volume of the simulation cell. These advances, as well as the ever-increasing body of experimental data upon which simulations can be validated, demonstrate that improvement of potential energy functions is a never ending process which must be revisited regularly.

The CHARMM (Chemistry at HARvard Molecular Mechanics) all-atom potential energy function for phospholipids, first published in 1996 and referred to here as CHARMM22,[4] continues to evolve. In 1997, it was extended to include unsaturated hydrocarbons.[5] Application of that force field to bilayers,[6−8] micelles,[9] and protein−lipid complexes[10] showed it to reproduce a variety of experimental observables; however, problems were evident. In simulations of a dipalmitoylphosphatidylcholine (DPPC) bilayer, order parameters for the carbon adjacent to the carbonyl group did not agree with experiment and the gauche fraction in the aliphatic tails was underestimated.[7] Concerning the headgroups, use of CHARMM22 was shown to yield densities that were too high when applied to a crystal simulation of glycerolphosphorylcholine (GPC).[11] Motivated by these limitations, additional optimization of several aspects of the CHARMM22 all-atom lipid parameters was undertaken.

In the following we present an overview of improvements made to the lipid force field over the past several years. These include enhancements to specific aspects of the force field that have been previously published,[12,13] along with new changes presented below. Where appropriate, comparisons are made between CHARMM22 and the new force field. The fully revised force field is then applied to an 11 ns simulation of a DPPC bilayer, results of which are compared to a variety of experimental data. The new all-atom lipid force field will be referred to as CHARMM27, based on the initial version of CHARMM with which the force field was released, and has been designed to be consistent with the CHARMM22 force-field for proteins[14] and the CHARMM27 force field for nucleic acids.[15,16] The CHARMM27 force field is included in its entirety in the Supporting Information or can be obtained from the following web page: www.pharmacy.umaryland.edu/∼alex. The program CHARMM,[17,18] which includes the entire CHARMM all-atom

* Address correspondence to: A. D. MacKerell Jr., Department of Pharmaceutical Sciences, School of Pharmacy,University of Maryland, 20 North Pine Street, Baltimore MD 21201. Telephone 410-706-7442. Fax 410-706-0346. E-mail alex@outerbanks.umaryland.edu

10.1021/jp0007843 CCC: $19.00
Published on Web 07/18/2000

biomolecular force field, may be obtained via email to marci@tammy.harvard.edu.

Methods

All calculations were performed with the program CHARMM.[17,18] Small molecule calculations were performed with no cutoff of the nonbond interactions with minimizations performed via the Newton−Raphson method to a gradient of 10^{-6} kcal/mol/Å. Potential energy surfaces were obtained by harmonically constraining the specified dihedral with a force constant of 10 000 kcal/mol/degree followed by complete minimization of the remainder of the system. Condensed-phase calculations were performed using periodic boundary conditions (PBC) in the isobaric, isothermal (NPT) ensemble using the Langevin-piston algorithm.[3] Alkane and lipid simulations were performed enforcing cubic and tetragonal symmetries, respectively (i.e., all lattice angles fixed at 90°), with only the *z* direction (bilayer normal) being flexible in the lipid simulation. Electrostatic interactions were calculated via the PME method,[1] using a kappa value of 0.30 and a fast-Fourier grid density of ca. 1 $Å^{-1}$. Cutoffs for the real space portion of the PME calculation and for truncation of the LJ interactions were 10 Å with the LJ interactions smoothed via a switching function over the range of 8 to 10 Å. SHAKE[19] was used to constrain all covalent bonds involving hydrogens and an integration time step of 2 fs was used. Nonbond lists were updated heuristically. A detailed description of the protocol employed in the lipid bilayer simulation is given in ref 7.

Results and Discussion

Phosphate Moiety. As discussed above, calculations showed the CHARMM22 model of GPC to overestimate the density of the crystal when subjected to an NPT molecular dynamics (MD) simulation. Those results pointed toward the need to improve the headgroup parameters, including those of the phosphate moiety. Alterations of the phosphate parameters, however, had to be performed while simultaneously taking into account their influence on the CHARMM22 all-atom nucleic acid force field.[20]

Initial optimization of the phosphate moiety concentrated on the torsional parameters that dictate the relative energies of the g,g, g,t, and t,t conformers of dimethyl phosphate (DMP) along with the barriers between those minima, as previously presented.[13] In that work, quantum mechanics (QM) calculations on DMP showed the presence of a single water molecule hydrating the molecule to significantly lower the relative energy of the g,t conformer. Later QM studies using the IPCM solvation model [21] have confirmed that result (A. D. MacKerell, Jr., unpublished results). Considering the hydrated nature of the phosphate group in lipids as well as in nucleic acids, a series of torsional parameters were developed that yielded gradually lower relative energies of the g,t conformer. Application of these parameters to simulations of duplex DNA in solution showed the sets with a lower relative energy of the g,t conformer to yield improvements in the equilibrium between the A and B forms of DNA, a problem that was present in the CHARMM22 all-atom nucleic acid parameters.[22,23] The set with the lowest relative energy of the g,t conformer was selected for the CHARMM27 force fields.

The second change in the phosphate moiety force field involved the partial atomic charges. As previously discussed in the context of the nucleic acid force field,[15] the interaction energies of different orientations of an individual water molecule with DMP were too favorable for the anionic oxygens and not favorable enough for the ester oxygens as compared to ab initio HF/6-31G(d) data. Adjustment of the partial atomic charges, shifting 0.02 e from the anionic oxygens to the ester oxygens, corrected this problem. Application of these charges to simulations of duplex DNA showed the hydration numbers of the anionic and ester oxygens to be in satisfactory agreement with experimental data.[16]

This combination of changes in the partial atomic charges and torsional parameters for the phosphate moiety have been tested in crystal simulations of GPC and cyclopentylphosphorylcholine (CPC) monohydrate.[24] In both cases, where CHARMM22 had overestimated the density of the GPC and CPC crystals by 10 and 11%, respectively, CHARMM27 led to improvements. For GPC the density was 6% too large, while it was only 3% too large for CPC. Thus, alterations in the phosphate force field that yielded improvements in the treatment of nucleic acids also led to improved treatment of the phospholipid headgroups, as judged by crystal calculations.

Aliphatic Moiety. The hydrocarbon torsional potential is critical in determining the structure of the bilayer interior, a topic that has received a great deal of attention from those carrying out molecular simulations. As discussed above, bilayer simulations indicated that the gauche fraction in the fatty acid chains was significantly underestimated as compared to experiment. For example, the liquid crystalline DPPC bilayer simulations of Feller et al. showed that, averaged over the thirteen individual dihedrals in each chain, the gauche fraction was 0.19 or 2.5 gauche defects per palmitic acid chain, approximately one less than experiment.[7] While such deficiencies are strongly indicative of limitations in the torsional parameters in the force field, chain conformations in lipids may also be affected by the membrane environment (as demonstrated by the observation that the number of gauche defects at the end of the fatty acid chain is typically greater than near the middle). Thus, the low gauche population observed in the lipid bilayer simulation could have been due to incorrect packing of molecules within the membrane, indicative of limitations in the LJ parameters, or due to errors in the torsional parameters. As discussed below, correction of both of these limitations contributed to improvement in the treatment of the aliphatic tails emphasizing the importance of balancing the bonded and nonbonded portions of the force field.

Beyond the lipid simulation data, other results indicated the presence of problems in the LJ parameters. Most worrisome was data showing that, in the case of ethane, changes in the carbon R_{min} term of over 0.5 Å could be compensated by the three remaining LJ parameters (i.e., C well depth, H well depth, and H R_{min}; see reference14 for definitions of the well depth (ϵ) and R_{min}), yielding virtually identical pure solvent properties.[25] This situation is representative of the parameter correlation problem where the underdetermined nature of parameters allows for a variety of combinations of parameters to reproduce target data. To overcome this limitation, a novel approach for the optimization of LJ parameters was developed and applied to hydrocarbons.[12] From this work, a new set of LJ parameters was developed that yielded satisfactory agreement with experimental data for short-chain alkanes both as pure solvents as well as aqueous solutes.

To test the adjusted hydrocarbon parameters in the context of a model system appropriate to lipids, hexadecane pure solvent simulations were performed. Table 1presents results from the CHARMM22 parameters, the present parameters, and an intermediate parameter set, along with the experimental data. Also included in Table 1 are the relative energies of the gauche conformer of butane for the three potentials and from high-

TABLE 1: Comparison of Hexadecane Pure Solvent Properties for Three Different Parameter Sets

parameter set	ΔH_{vap}[a,b]	mol. vol.[a]	gauche P. E.	fraction gauche
experimental	19.45	486.4	0.65[c]	0.35[d]
CHARMM22	23.72	483.2 ± 2.8	0.85	0.13 ± 0.04
Y&M[e]	19.58	496.6 ± 0.9	0.83	0.22 ± 0.02
CHARMM27	18.24	499.1 ± 0.7	0.63	0.34 ± 0.01

[a] Energies in kcal/mol and molecular volume in Å^3. [b] Hexadecane NPT/PBC simulations performed at 293 K with ΔH_{vap} values that include a long range correction for the LJ term. Experimental value from reference 44. [c] Ab initio data at the CCSD/cc-pVTZ level using the MP2/6-311G(2df,p) geometry from Smith and Jaffe.[26] [d] Based on tridecane ($C_{13}H_{28}$).[45] [e] Y&M is the force field published by Yin and MacKerell.[12]

level ab initio calculations. As may be seen, CHARMM22 significantly overestimated the heat of vaporization and underestimated the fraction gauche as compared to experiment. Adjustment of the LJ parameters, with only a small change in the gauche potential energy, indicated as Y&M in Table 1, yielded improvements in both the heat of vaporization and in the fraction gauche, though the molecular volume became slightly too high. Notable was the improvement in the fraction gauche, while only a small change in the butane gauche energy occurred. This outcome indicates the linkage between the bonded and nonbonded portions of the force field, and the importance of properly balancing the two aspects.

While improvement due to adjustment of the LJ parameters is evident, there was a need for further improvement in both the thermodynamic and conformational properties. Most obvious was the need to decrease the relative gauche potential energy in order to increase the fraction gauche. Facilitating the decision to decrease the gauche energy were high-level ab initio calculations on butane and hexane.[26] Those calculations indicated the relative energy of the gauche conformer of butane to be approximately 0.6 kcal/mol, compared to earlier experimental estimates in the range of 0.75−0.97 kcal/mol (see Supporting Information of Yin and MacKerell[12] for primary references). Accordingly, reoptimization of the torsional parameters was undertaken.

Reoptimization of the aliphatic torsional parameters focused on the energetics of butane and hexane as well as the overall shape of the butane CCCC dihedral potential energy surface. Presented in Table 2 are the relative energies of butane and selected hexane conformers and in Figure 1 the CCCC dihedral potential energy surfaces for butane are presented. Note that the conformers presented for hexane correspond to those studied by Smith and Jaffe.[26] For butane, analysis of Table 2 shows the CHARMM27 results to generally be in better agreement with the ab initio data as compared to CHARMM22. The only exception occurs with the cis energy barrier, which is lower in CHARMM27 as compared to both the ab initio and CHARMM22 results. Sacrificing the cis energy, a conformation which will not be significantly sampled in MD simulations, was performed to allow for better reproduction of the shape of the butane surface, especially in the region of the gauche minimum (Figure 1). Consistent with the butane data, the CHARMM27 results are in satisfactory agreement with the ab initio data for hexane. Interestingly, CHARMM22, which was not explicitly parameterized for hexane, is also in good agreement with the ab initio data, although the gauche (i.e., t,t,g) energy significantly differs.

Testing the influence of the changes in the torsional parameters upon going from CHARMM22 to CHARMM27 was again performed via a hexadecane pure solvent simulation (Table 1). The CHARMM27 result, which includes both the improved LJ and torsional parameters, is seen to somewhat overestimate the heat of vaporization and molecular volume with the fraction gauche being in excellent agreement with the experimental data. While the improvement in the fraction gauche data was anticipated, the significant alteration in the heat of vaporization was unexpected, again emphasizing the linkage between the bonded and nonbonded portions of the force field.

TABLE 2: Relative Potential Energies of Selected Conformers of Butane and Hexane from Ab Initio and Empirical Calculations[a]

	A. I.	C22	Diff	C27	Diff
		Butane			
t,g barrier					
energy	3.31	3.48	0.17	3.33	0.02
gauche					
CCCC	62.80	66.52	3.72	62.26	−0.54
energy	0.59	0.85	0.26	0.63	0.04
cis					
energy	5.48	5.25	−0.23	4.96	−0.52
		Hexane			
t,g barrier					
energy	2.92	2.61	−0.31	3.31	0.39
t,t,g minimum					
CCCC	66.40	69.06	2.66	62.60	−3.80
energy	0.52	0.08	−0.44	0.56	0.04
cis barrier					
energy	5.63	4.92	−0.71	4.98	−0.65

[a] Potential energies in kcal/mol and dihedrals (i.e., CCCC) in degrees. Butane ab initio (A. I.) data at the CCSD(T)/cc-pVTZ//MP2/6-311G(2df,p) level and hexane ab initio data at the MP2/6-311++G(**)//SCF/6-311++G(**) level of theory. For the butane and hexane ab initio t,g barriers, the dihedral angles were 119.5° and 119.3°, respectively, while the empirical values were 120°. Cis barriers were constrained to 0° in all cases. See original reference for additional information on the ab initio data.[26]

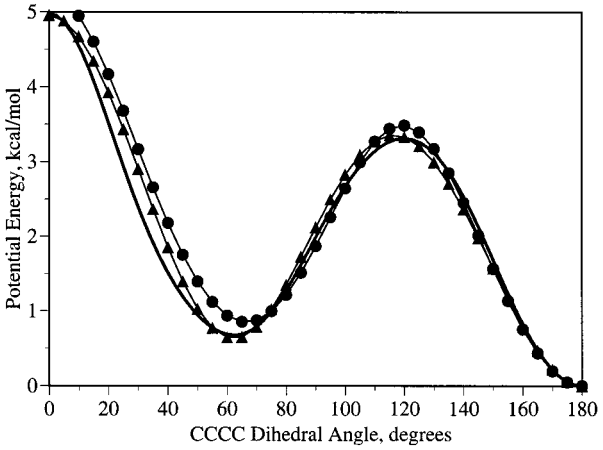

Figure 1. Potential energy of butane as a function of the C−C−C−C dihedral angle from MP2/6-311G(2df,p) QM calculations[26] and empirical calculations using the CHARMM22 (●) and CHARMM27 (▲) force fields.

DPPC Bilayer Simulation. Ultimate verification of a biomolecular force field is its success in reproducing experimental data on the biological system of interest. Accordingly, simulations of a DPPC bilayer in the liquid-crystal phase were undertaken using CHARMM27. This system has the advantage of being the subject of a variety of experimental studies, as well as previously being subjected to MD simulations using the CHARMM22 force field.

The experimental quantity that is most often compared with simulation in validating the bilayer interior is the deuterium order parameter, S_{CD}, profile. The order parameter is determined experimentally from the measured quadrapolar splitting

$$\Delta\nu_Q = \frac{3}{4}\left(\frac{e^2qQ}{h}\right)S_{CD} \quad (1)$$

where the term in parentheses is the quadrapolar coupling constant. The order parameter is calculated in the simulation from the angle, θ, between the C−H bond vector and the bilayer normal (z direction) by

$$S_{CD} = \left\langle \frac{3}{2}\cos^2\theta - \frac{1}{2} \right\rangle \quad (2)$$

where the brackets denote an averaging over all lipids and over time. The order parameter can be calculated for each carbon atom along the fatty acid chain, providing information on the average orientation of each methylene segment. Figure 2 presents calculated order parameters from an 11 ns simulation of a fluid-phase DPPC bilayer[27] along with experimentally measured values. Excellent agreement is seen between simulation and experiment, e.g., the discrepancies with experiment are comparable to the differences in experimental order parameters reported by individual laboratories. Yet unresolved, however, is the previously mentioned problem with the order parameters calculated for carbon 2 of each fatty acid chain. Table 3 shows that the C2 order parameter calculated for the sn-1 chain is significantly smaller in magnitude than is observed experimentally, and the unique order parameter observed for each of the two hydrogens bonded to C2 of the sn-2 chain is not reproduced in the simulation. In this respect there is no improvement observed when moving from CHARMM22 to CHARMM27. We are currently working to address this problem.

Figure 3 shows the probability distribution for rotation about the central dihedral of the fatty acid chains. The location of the gauche maxima is shifted from ~71° in CHARMM22 to ~63° in CHARMM27. Additionally, the gauche fraction is increased to an average of 0.26 for the 13 chain dihedrals (compared to 0.19 with the previous parameter set), or approximately 3.5 gauche defects per chain. These values obtained with the CHARMM27 force field are in good agreement with experimental estimates obtained from dilatometry/calorimetry,[28] NMR,[29] and IR spectroscopy.[30,31]

The electron density distribution through the bilayer has been studied experimentally using X-ray diffraction techniques. In Figure 4, the electron density calculated from the simulation trajectory is seen to be in excellent agreement with experimental density profiles obtained by Nagle and co-workers.[32] For the best resolved feature, the location of the headgroup peaks, the simulation results lie between the two experimental curves (the difference between the experimental curves is related to differences in data analysis). For the width of both the methylene plateau and methyl trough, the simulation results again are found midway between the two experimental estimates. Another source of experimental data on the location of lipid segments along the bilayer normal are neutron scattering experiments on isotopically labeled carbon atoms.[33,34] Differences between the simulation and neutron data for the 9 carbon positions studied experimentally average less than 1 Å, well within the experimental precision (not shown). Application of the CHARMM22 force field to DPPC yielded electron density profiles[7] similar to those in Figure 4; however, those simulations were run for an order of magnitude less than the present simulation, making more rigorous comparisons difficult.

Recently, Gawrisch and co-workers have measured NOESY cross-relaxation rates for DPPC bilayers, providing a quantitative measure of both lateral structure with the membrane and of membrane dynamics.[35,36] In a recent publication, we have compared cross-relaxation rates calculated from the present 11 ns DPPC bilayer simulation and found very good agreement with the experimental values of Gawrisch and co-workers.[27]

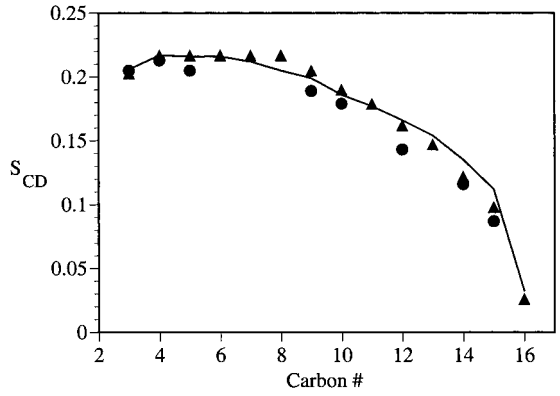

Figure 2. Deuterium order parameters, S_{CD}, for the sn-2 chain of DPPC. The solid line indicates the CHARMM27 simulation results, the (●) symbols are the experimental results of Douliez et al.,[47] and the (▲) symbols are the experimental results of Seelig and Seelig.[46]

TABLE 3: Experimental and Calculated Order Parameters for Aliphatic Carbon-2 of DPPC

source	C2-sn1	C2-sn2a	C2-sn2b
expt 1[a]	−0.216	−0.150	−0.094
expt 2[b]	−0.213	−0.142	−0.097
CHARMM22	−0.157	−0.161	−0.144
CHARMM27	−0.135	−0.165	−0.158

[a] Experimental data set 1 from Seelig and Seelig.[46] [b] Experimental data set 2 from Douliez et al.[47]

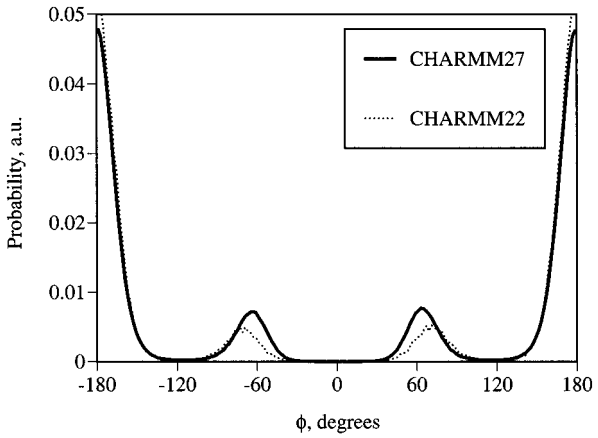

Figure 3. Probability distribution for rotation about the C8−C9−C10−C11 dihedral angle of the palmitic acid chains. The solid and dashed lines are the CHARMM27 and CHARMM22 results, respectively.

Conclusion

Presented is a revision of the CHARMM all-atom force field for lipid simulation. While the CHARMM22 force field was successful in many respects, there were a number of deficiencies, as discussed above, which motivated the present work. In essence, application of the force field has itself become part of the parameter optimization process. By using information from simulations of different systems by different laboratories in the optimization process, a broader range of goal data can be used for the parameter adjustment. This approach has recently been applied to other force fields[14,37,38] and has been discussed in detail.[15] It is expected that the inclusion of biomolecular simulations as an explicit step in the parameter optimization process will continue in the future.

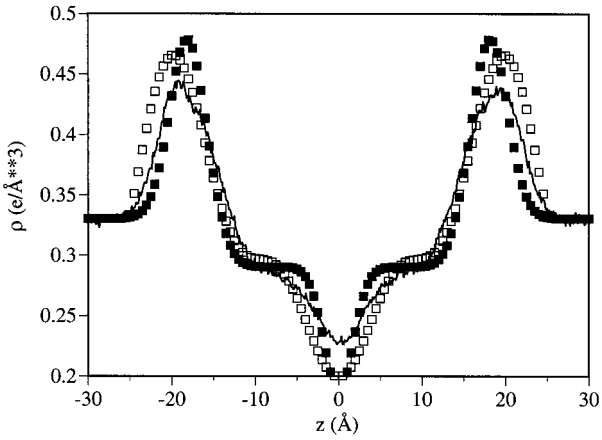

Figure 4. Electron density as a function of position along the membrane normal. The solid line gives the simulation result, the filled and open symbols are from Figures 9 and 6, respectively, of reference 32.

Of note in the present study was the influence of the bonded parameters on calculated thermodynamic properties and, vice versa, the influence of the nonbonded parameters on the conformational propeties (Table 1). Such results emphasize the importance of obtaining the proper balance between the bonded and nonbonded portions of a force field. To obtain such balance, an iterative approach to parameter optimization must be undertaken. A detailed account of the iterative approach used in optimization of the CHARMM all-atom force fields is presented elsewhere.[25]

A possible weakness of the present force field is the disagreement with experiment for the heat of vaporization and molecular volume of hexadecane (6.2% and −2.6%, respectively, Table 1), even though the changes in the hydrocarbon LJ and torsional parameters produced significant improvement over CHARMM22 with respect to the heat of vaporization. This discrepancy is significantly larger than results for ethane, propane, and butane[12] and is consistent with published reports that parameters for extended-chain *n*-alkanes cannot be directly transferred from the short-chain *n*-alkanes.[39,40] Accordingly, it may be deemed appropriate to optimize alkane parameters for lipid simulations, in particular the LJ parameters, based on long-chain *n*-alkanes. Such an approach, however, makes it difficult to maintain compatibility with hydrocarbons on other molecules when performing simulations of heterogeneous systems (e.g., protein−lipid systems). While more studies are needed to rigorously address this compatibility issue, with CHARMM27 we have possibly sacrificed the long-chain *n*-alkane pure-solvent properties in order to maintain the overall consistency of the force field. It should be noted that the discrepancies in heat of vaporization and molecular volume may also be attributable to the neglect of long range LJ interactions in the CHARMM calculation of pressure. Inclusion of these forces will decrease the pressure, as they are solely attractive in nature, thus decreasing the system volume. Decreasing system volume would directly improve agreement for molecular volume and would likely improve the heat of vaporization by lowering the potential energy of the liquid state. Thus, given the uncertainty in the pressure calculation and the stated goal of maintaining parameter compatibility, we find these results acceptable.

The CHARMM27 all-atom force field represents the next step in the continued extension and refinement of the CHARMM all-atom biomolecular force field. This force field now includes proteins,[14] nucleic acids,[15,16] carbohydrates (John Brady, personal communication), and lipids, as well as a variety of small molecules[41] and enzyme cofactors.[42] Accordingly, the force field is useful for computational studies of the heterogeneous systems that are common in biochemistry. A recent example includes a study of a DNA-DMPC-DMTAP ternary system performed using the CHARMM27 lipid and nucleic acids force fields.[43] Combined with increased computational resources it is hoped that the present lipid force field will facilitate simulations of biologically interesting membrane systems.

Acknowledgment. A.D.M., Jr. expresses his appreciation for computational support from the NPACI HPC and DoD HPC resources, and financial support from the NIH (GM51501). S.E.F. expresses his appreciation for financial support from the National Science Foundation through grant MCB-9896211.

Supporting Information Available: Included is a table describing the chemical entities included in the CHARMM27 lipid force field along with the CHARMM27 lipid topology and parameter files in CHARMM format. This material is available free of charge via the Internet at http://pubs.acs.org, or at www.pharmacy.umaryland.edu/∼alex.

References and Notes

(1) Darden, T. A.; York, D.; Pedersen, L. G. *J. Chem. Phys.* **1993**, *98*, 10089−10092.
(2) Martyna, G. J.; Tobias, D. J.; Klein, M. L. *J. Chem. Phys.* **1994**, *101*, 4177−4199.
(3) Feller, S. E.; Zhang, Y.; Pastor, R. W.; Brooks, R. W. *J. Chem. Phys.* **1995**, *103*, 4613−4621.
(4) Schlenkrich, M.; Brickmann, J.; MacKerell, A. D., Jr.; Karplus, M. Empirical Potential Energy Function for Phospholipids: Criteria for Parameter Optimization and Applications. In *Biological Membranes: A Molecular Perspective from Computation and Experiment*; Merz, K. M., Roux, B., Eds.; Birkhaüser: Boston, 1996; pp 31−81.
(5) Feller, S. E.; Yin, D.; Pastor, R. W.; MacKerell, A. D., Jr. *Biophys. J.* **1997**, *73*, 2269−2279.
(6) Venable, R. M.; Zhang, Y.; Hardy, B. J.; Pastor, R. W. *Science* **1993**, *262*, 223−226.
(7) Feller, S. E.; Venable, R. M.; Pastor, R. W. *Langmuir* **1997**, *13*, 6555−6561.
(8) Gambu, I.; Roux, B. *J. Phys. Chem. B* **1997**, *101*, 6066−6072.
(9) MacKerell, A. D., Jr. *J. Phys. Chem.* **1995**, *99*, 1846−1855.
(10) Woolf, T. B.; Roux, B. *Proc. Natl. Acad. Sci. U.S.A.* **1994**, *91*, 11631−11635.
(11) Tu, K.; Tobias, D. J.; Klein, M. L. *J. Phys. Chem.* **1995**, *99*, 10035−10042.
(12) Yin, D.; MacKerell, A. D., Jr. *J. Comput. Chem.* **1998**, *19*, 334−348.
(13) MacKerell, A. D., Jr. *J. Chim. Phys.* **1997**, *94*, 1436−1447.
(14) MacKerell, A. D., Jr.; Bashford, D.; Bellott, M.; Dunbrack, R. L., Jr.; Evanseck, J.; Field, M. J.; Fischer, S.; Gao, J.; Guo, H.; Ha, S.; Joseph, D.; Kuchnir, L.; Kuczera, K.; Lau, F. T. K.; Mattos, C.; Michnick, S.; Ngo, T.; Nguyen, D. T.; Prodhom, B.; Reiher, W. E., III.; Roux, B.; Schlenkrich, M.; Smith, J.; Stote, R.; Straub, J.; Watanabe, M.; Wiorkiewicz-Kuczera, J.; Yin, D.; Karplus, M. *J. Phys. Chem. B* **1998**, *102*, 3586−3616.
(15) Foloppe, N.; MacKerell, A. D., Jr. *J. Comput. Chem.* **2000**, *21*, 86−104.
(16) MacKerell, A. D., Jr.; Banavali, N. *J. Comput. Chem.* **2000**, *21*, 105−120.
(17) Brooks, B. R.; Bruccoleri, R. E.; Olafson, B. D.; States, D. J.; Swaminathan, S.; Karplus, M. *J. Comput. Chem.* **1983**, *4*, 187−217.
(18) MacKerell, A. D., Jr.; Brooks, B.; Brooks, C. L., III.; Nilsson, L.; Roux, B.; Won, Y.; Karplus, M. CHARMM: The Energy Function and Its Parameterization with an Overview of the Program. In *Encyclopedia of Computational Chemistry*; Schleyer, P. v. R., Clark, N. L. A., T., Gasteiger, J., Kollman, P. A., Schaefer, H. F., III, Schreiner, P. R. S, Ed.; John Wiley & Sons: Chichester, 1998; Vol. 1; pp 271−277.
(19) Ryckaert, J. P.; Ciccotti, G.; Berendsen, H. J. C. *J. Comput. Phys.* **1977**, *23*, 327−341.
(20) MacKerell, A. D., Jr.; Wiórkiewicz-Kuczera, J.; Karplus, M. *J. Am. Chem. Soc.* **1995**, *117*, 11946−11975.
(21) Tomasi, J.; Persico, M. *Chem. Rev.* **1994**, *94*, 2027−2094.
(22) Feig, M.; Pettitt, B. M. *Biophys. J.* **1998**, *75*, 134−149.
(23) Feig, M.; Pettitt, B. M. *J. Phys. Chem. B* **1997**, *101*, 7361−7371.
(24) Tobias, D. J.; Tu, K.; Klein, M. L. *J. Chim. Phys.* **1997**, *94*, 1482−1502.

(25) MacKerell, A. D., Jr. Atomistic Models and Force Fields. In *Computational Biochemistry and Biophysics*; Becker, O. M., MacKerell, A. D., Jr., Roux, B., Watanabe, M., Eds.; Marcel Dekker: New York, in press.
(26) Smith, G. D.; Jaffe, R. L. *J. Phys. Chem.* **1996**, *100*, 18718−18724.
(27) Feller, S. E.; Huster, D.; Gawrisch, K. *J. Am. Chem. Soc.* **1999**, *121*, 8963.
(28) Nagle, J. F.; Wilkinson, D. A. *Biophys. J.* **1978**, *23*, 159.
(29) Schindler, H.; Seelig, J. *Biochemistry* **1975**, *14*, 2283.
(30) Mendelsohn, R.; Davis, A. M.; Brauner, J. W.; Schuster, H. F.; Dluhy, R. A. *Biochemistry* **1989**, *28*, 8934.
(31) Casal, H. L.; McElhaney, R. N. *Biochemistry* **1990**, *29*, 5423.
(32) Nagle, J. F.; Zhang, R.; Tristram-Nagle, S.; Sun, W.; Petrache, H.; Suter, R. M. *Biophys. J.* **1996**, *70*, 1419.
(33) Büldt, G.; Gally, H. U.; Seelig, J.; Zaccai, G. *J. Mol. Biol.* **1979**, *134*, 673.
(34) Zaccai, G.; Büldt, G.; Seelig, A.; Seelig, J. *J. Mol. Biol.* **1979**, *134*, 693.
(35) Huster, D.; Arnold, K.; Gawrisch, K. *J. Phys. Chem. B* **1999**, *103*, 243.
(36) Huster, D.; Gawrisch, K. *J. Am. Chem. Soc.* **1999**, *121*, 1992.
(37) Langley, D. R. *J. Biomol. Struct. Dyn.* **1998**, *16*, 487−509.
(38) Cheatham, T. E., III.; Cieplak, P.; Kollman, P. A. *J. Biomol. Struct. Dyn.* **1999**, *16*, 845−861.
(39) Berger, O.; Edholm, O.; Jahnig, F. *Biophys. J.* **1997**, *72*, 2002−2013.
(40) Chiu, S. W.; Clark, M. M.; Jakobsson, E.; Subramaniam, S.; Scott, L. H. *J. Phys. Chem. B* **1999**, *103*, 6323−6327.
(41) Yin, D. Parametrization for Empirical Force Field Calculations & A Theoretical Study of Membrane Permeability of Pyridine Derivatives. Ph.D. Thesis, University of Maryland, 1997.
(42) Pavelites, J. J.; Gao, J.; Bash, P. A.; MacKerell, A. D., Jr. *J. Comput. Chem.* **1997**, *18*, 221−239.
(43) Bandyopadhyay, S.; Tarek, M.; Klein, M. L. *J. Phys. Chem. B* **1999**, *103*, 10075−10080.
(44) Majer, V.; Svoboda, V. *Enthalpies of Vaporization of Organic Compounds: A Critical Review and Data Compilation*; Blackwell Scientific Publications: Oxford, 1985.
(45) Holler, F.; Callis, J. B. *J. Phys. Chem.* **1989**, *93*, 2053−2058.
(46) Seelig, A.; Seelig, J. *Biochemistry* **1974**, *13*, 4839−4845.
(47) Douliez, J.-P.; Léonard, A.; Dufourc, E. J. *Biophys. J.* **1995**, *68*, 1727−1739.